# 23 Future Perspective in Abdominal Ultrasound

Junji Machi, Fuminori Moriyasu, Shigeki Arii, Masahiko Yano, and Emi Saegusa-Beecroft

## History of the Use of Ultrasound by Surgeons

The history of surgeon-performed ultrasound went back to a half century ago; surgeons in the United States were behind in the use of ultrasound. In European and Asian countries, surgeons started ultrasound examination by themselves as preoperative and intraoperative tools in the 1970s. One of the examples is an ultrasound probe specifically for intraoperative use which was created by Dr. Masatoshi Makuuchi to evaluate and localize nonpalpable liver tumors in the operative field in the mid-1970s.

In the United States, one of the earliest surgeon-performed ultrasound examinations was in the operating room. Dr. Bernard Sigel, a general surgeon and a pioneer of intraoperative ultrasound (IOUS), introduced this modality during surgery in 1979 for intraoperative diagnosis of biliary calculi. In the early 1980s, IOUS was employed during neurosurgery, endocrine surgery, and cardiovascular surgery. Since 1980, the Sigel's group (which Junji Machi joined) expanded the application of IOUS to various fields including hepatobiliary, pancreatic, and other abdominal surgery. Although benefits of IOUS were clearly reported, gaining acceptance of IOUS among surgeons was slow in the 1980s, particularly in the United States.

However, in the mid-1990s, many surgeons recognized the value of IOUS during surgical procedures, and with the availability of various types of IOUS and laparoscopic ultrasound (LUS) probes, the use of ultrasound has become more widespread during a variety of operations, especially for abdominal surgery. In certain operations such as hepatectomy, IOUS is presently considered as an essential modality, making liver surgery without IOUS suboptimal.

In addition, in the 1990s, surgeons started ultrasound examinations in the emergency room for patients with trauma and in the office for breast and thyroid evaluation with ultrasound-guided needle biopsy or aspiration and for abdominal examination pre- and postoperatively. Vascular surgeons were at that time already using ultrasound in their noninvasive vascular laboratory.

Because of expansion and future expectation of increased use of ultrasound by surgical practices, the American Board of Surgery made an announcement in the mid-1990s that during surgical training, residents should learn ultrasound examination. Soon after that, the American College of Surgeons set up a team of surgeon-sonographers as National Ultrasound Faculty and provided postgraduate skill courses in various fields such as trauma, breast, vascular, thyroid/parathyroid, and ICU cardiothoracic in addition to abdominal

J. Machi, MD, PhD, FACS (✉)
Department of Surgery, John A. Burns School of Medicine, University of Hawaii and Kuakini Medical Center, Honolulu, HI, USA

Noguchi Medical Research Institute, JADECOM-NKP GME Center Tokyo Bay, Urayasu-Ichikawa Medical Center, (Noguchi Hideyo Memorial International Hospital), Urayasu, Chiba, Japan
e-mail: junji@hawaii.edu

F. Moriyasu, MD, PhD
Department of Gastroenterology and Hepatology, Tokyo Medical University, 6-7-1 Nishishinjuku, Shinjuku-ku, Tokyo, 160-0023, Japan
e-mail: moriyasu@rb4.so-net.ne.jp

S. Arii, MD, PhD
Department of Hepato-Biliary-Pancreatic Surgery, Tokyo Medical and Dental University, 1-5-45, Yushima, Bunkyo-ku, Tokyo, 113-8510, Japan
e-mail: sh-arii@hamamatsuh.rofuku.go.jp

M. Yano
Ultrasound Systems Division, Ultrasound Systems Development Department, Tokyo Medical Systems Corporation, 1385 Shimoishigami, Otawara-Shi, Tochigi, 324-8550, Japan
e-mail: masahiko.yano@toshiba.co.jp

E. Saegusa-Beecroft, MD, PhD
Department of Surgery, JABSOM, University of Hawaii and Kuakini Medical Center, 405 N. Kuakini Street, Suite 601, Honolulu, HI 96817, USA
e-mail: esaegusa@hawaii.edu

**Electronic supplementary material** The online version of this chapter (doi:10.1007/978-1-4614-9599-4_23) contains supplementary material, which is available to authorized users. Videos can also be accessed at http://www.springerimages.com/videos/978-1-4614-9598-7

E.J. Hagopian, J. Machi (eds.), *Abdominal Ultrasound for Surgeons*, DOI 10.1007/978-1-4614-9599-4_23, © Springer Science+Business Media New York 2014

ultrasound including IOUS, LUS, and transabdominal ultrasound (TAUS). Currently, there are ultrasound courses for residents and instructors as well. Other societies in the United States including Society of American Gastrointestinal and Endoscopic Surgeons and Americas Hepato-Pancreato-Biliary Association are holding abdominal ultrasound courses with hands-on sessions. Taking such courses is helpful for surgeons, especially for the ultrasound neophyte, who are interested in getting started in surgical ultrasound.

## Perspective of Surgeon-Performed Ultrasound

Surgeons are currently using ultrasound in a variety of surgical settings such as the office, the ward bedside, the emergency room, the intensive care unit (by means of TAUS), and the endoscopic suite (by means of endoscopic or endorectal ultrasound (EUS)) as well as in the operating room (by means of IOUS and LUS). The state of the art of surgeon-performed abdominal ultrasound is described in this book. How about the future of abdominal ultrasound?

In the 1980s, the standard ultrasound was performed by 2-dimensional (2D) real-time B-mode ultrasound. One renovation of ultrasound occurred in the early 1990s, when color Doppler and then power Doppler imaging was introduced. Color/power Doppler imaging displays blood flow in real-time color on B-mode gray-scale images and has been used during operation as well as in the radiology department. By offering blood flow information in addition to anatomical information, this modality enhances the efficacy of IOUS and LUS during general and cardiovascular surgery. Intraoperative color/power Doppler imaging can detect and localize smaller vessels, can promptly distinguish them from ductal structures and tissue spaces, and can confirm blood flow to organs after surgical operations such as transplantation or major organ resection. These capabilities improve reading of images of surgeon-performed ultrasound.

More uses of ultrasound in future during various procedures (intra-procedural ultrasound including IOUS and LUS) will be brought about by a combination of ultrasound and other technological advances and surgeons' interest and experience. Some predictable occurrences include expansion of ultrasound applications, improvement in instrumentation, and incorporation of new ultrasound technologies.

IOUS/LUS will be used by surgeons steadily and increasingly, along with more formal training in ultrasound for residents and surgeons. Having IOUS/LUS instruments always available in the operating room and having competent surgeons available performing IOUS/LUS will permit IOUS/LUS to become not just an occasional but an everyday tool for acquiring intraoperative information; it will allow surgeons to "see" organs and lesions in a new dimension. This is particularly true in the use of LUS because of ongoing broader applications of laparoscopic or minimally invasive operations.

New innovative ultrasound technologies will lead to further improvement in image resolution and deeper sound penetration of IOUS/LUS. More user-friendly probes and scanners for surgeons are being developed. New ultrasound technological developments, such as harmonic imaging with contrast agents (intravenous ultrasound contrast is not available yet for abdominal organs in the United States as of November 2013), will improve the diagnostic accuracy of IOUS/LUS. The refinement of 3-dimensional (3D) images will simplify IOUS and LUS for planning and guiding tumor ablation or organ resections, such as hepatectomy. Anatomical and pathological information provided by 3D IOUS/LUS will enable quicker and more assured IOUS/LUS-guided surgical procedures. Thereby, 3D images may increase the diagnostic confidence of the surgeons, which is often an obstacle for the broader usage of ultrasound.

Introduction and advances of various other medical or nonmedical technologies will continuously influence or alter imaging methods and surgical procedures. In addition, less and less invasive surgery with smaller access sites will keep surgeons' hands further away from organs, thus requiring more image guidance as seen in minimally invasive and percutaneous image-guided procedure. Therefore, there will be a less distinctive border between open and percutaneous interventional ultrasound; these ultrasound techniques can eventually be categorized as "intra-procedural ultrasound." Natural orifice transluminal endoscopic surgery (NOTES) is another newer surgical-endoscopic field, in which EUS will play a role. EUS-guided radiofrequency ablation of abdominal tumors is one example of NOTES. Eventually, many of the surgical procedures that have been done with open, laparoscopic, or percutaneous approaches may be performed by endoscopic approaches, which in many cases may be guided by EUS. As technology evolves, new advances in imaging methods and image-guided procedures including IOUS, LUS, and EUS should be carefully assessed to define its practical role and cost-effectiveness in future.

## Learning of Abdominal Ultrasound in Future

Performance of 2-dimensional real-time ultrasound images requires familiarity with how the position of the probe (transducer) relates to the image on the monitor screen. This probe-image orientation requires hand-eye coordination by the operator in order to understand where a particular anatomical region is shown on the screen. To acquire this type of orientation, the surgeon who is not familiar with the ultrasound probe and scan display on the monitor is well advised to practice ultrasound examination on a daily basis;

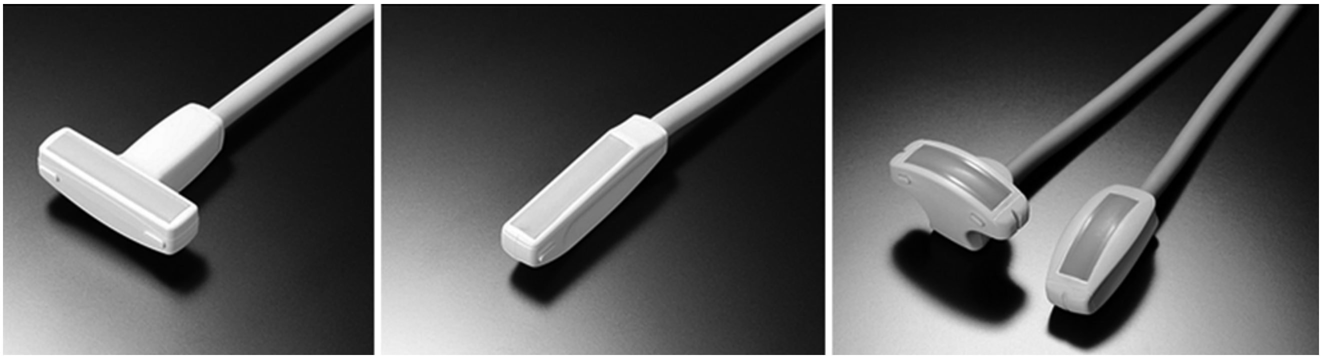

**Fig. 23.1** Various types of intraoperative ultrasound (IOUS) probes

"Scan, Scan, Scan" is probably the best way to learn ultrasound. Eventually, a surgeon becomes capable of creating 3-dimensional images in his or her brain from 2-dimensional images in real time.

Before or while clinically scanning patients (human being), "Scan" can be practiced using new tools such as phantoms and stimulators. Ultrasound phantoms are available for practicing TAUS, IOUS, and LUS scanning techniques. Ultrasound simulation systems can be used to learn EUS as well as IOUS. Virtual reality technology will continually advance so that more realistic simulation of TAUS/IOUS/LUS examinations as well as surgical procedures will become available. Computer-based ultrasound simulators will greatly help future education and training in abdominal ultrasound. For general surgeons, particularly hepatobiliary, pancreatic, and endocrine surgeons, surgical oncologists, and laparoscopic surgeons, it will become critically important to master abdominal ultrasound, particularly IOUS and LUS. Collaboration with radiologists may be important initially; however, I believe it is imperative that surgeons themselves eventually should perform surgical ultrasound such as IOUS and LUS.

## New and Promising Technology in Abdominal Ultrasound (Including Video Clips)

### Intraoperative Contrast-Enhanced Ultrasound

#### Applications

In 2007, Sonazoid® (microbubbles contained in the agent which remain stable when subject to ultrasonic sound waves, enabling continuous vascular and Kupffer imaging) was approved as an ultrasound contrast for clinical use in Japan. Since that time, the use of Sonazoid in surgical procedures has been attracting a great deal of attention.

In particular, imaging in the delayed phase approximately 10 min after the intravenous injection of Sonazoid is becoming a focus of interest. This imaging technique exploits the fact that Sonazoid is phagocytized by Kupffer cells. Since Kupffer cells are not present in malignant tumors such as HCCs and metastases, echoes from contrast medium are not observed in such lesions, which therefore appear black (anechoic-hypoechoic) in ultrasound images. Such images are referred to as Kupffer images. Kupffer images make it possible to assess a tumor and its degree of invasion before surgery and are also sometimes used to select the most appropriate surgical procedure. In addition, the use of high-frequency probes in Kupffer imaging enables the detection of hepatic metastases measuring 5 mm or less, which can contribute to more accurately determine prognosis and treatment options.

#### Setup and Imaging Conditions

High-frequency intraoperative probes such as those shown in Fig. 23.1 and an ultrasound system that supports contrast-enhanced imaging are required for examinations using Sonazoid. The MI (mechanical index) should be in the range from 0.1 to 0.15, and the frame rate should be approximately 15 fps to ensure real-time display and avoid the collapse of bubbles. Lower frequencies are generally the most suitable for the stable detection of bubble signals. However, when determining the optimal frequency, it should be kept in mind that there is a tradeoff between resolution and tissue signal detection. The focal point should be set at the inferior border of the region of interest or the inferior border of the field of view.

#### Clinical Usefulness

Kupffer imaging makes it possible to visualize the location, size, and shape of tumors that are difficult to visualize in B-mode images and at the same time allows the courses of vessels near tumors to be confirmed before resection. This is a great advantage for surgical application. As shown in Fig. 23.2, the difference between conventional B-mode and Kupffer images are obvious. The exact shape of the tumor, which cannot be determined accurately in the B-mode image, is clearly depicted in the Kupffer image.

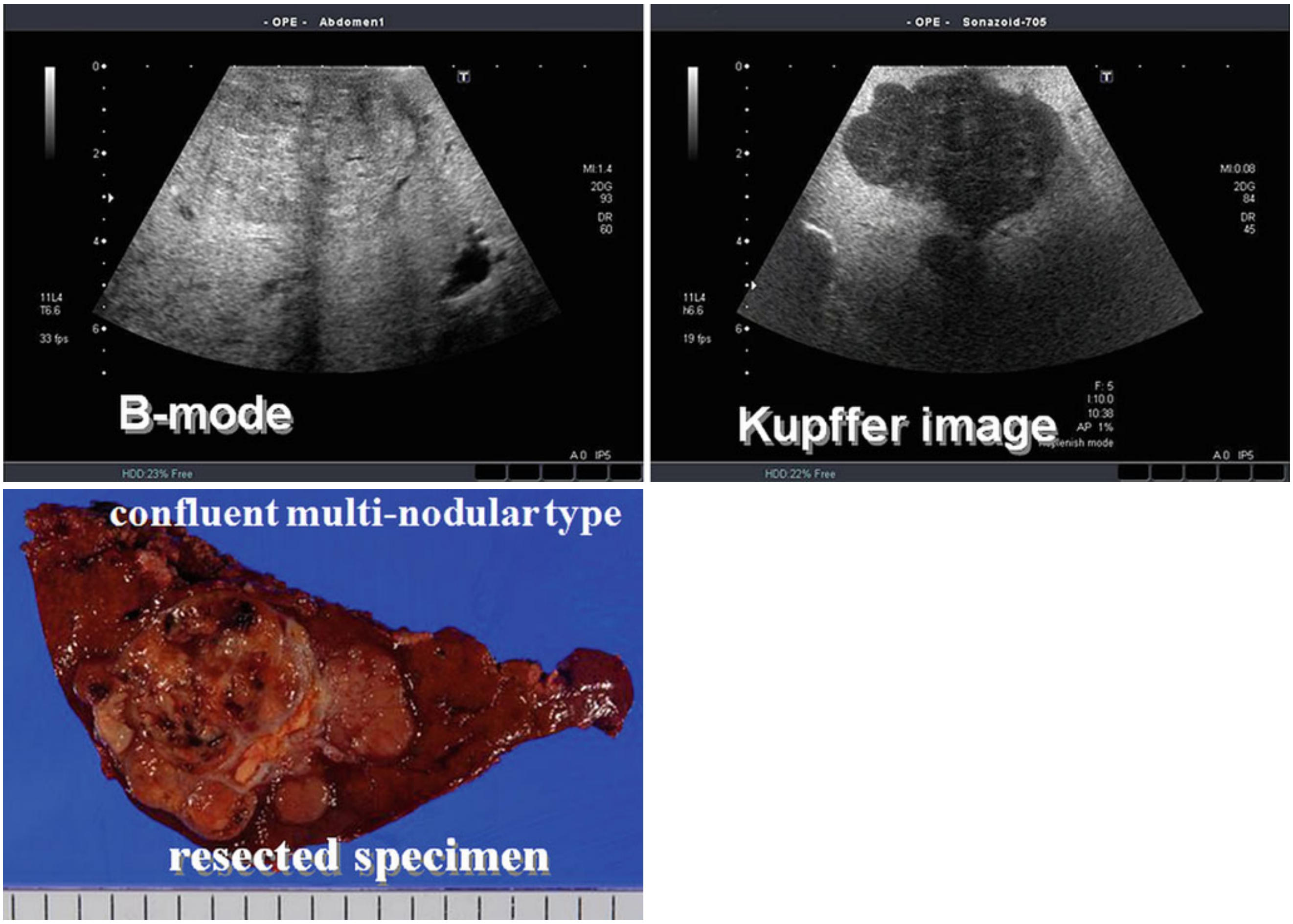


**Fig. 23.2** IOUS B-mode and Kupffer images of a malignant liver tumor with a resected specimen

Kupffer imaging is also useful for detecting small malignant lesions. Metastases measuring less than 5 mm cannot be often visualized by B-mode. Kupffer imaging, on the other hand, is able to detect smaller intrahepatic metastases, as shown in Fig. 23.3.

Attempts have also been made to assess the degree of tissue differentiation by observing the courses of vessels within the tumor in the vascular phase. When micro-flow imaging (MFI), which displays bubble motion as a summed residual image, is used, fine blood vessels exhibiting various degrees of differentiation can be observed within an HCC, as shown in Fig. 23.4 (see also Video 23.1). It has been found that well-differentiated carcinomas exhibit the so-called “cotton pattern” and moderately differentiated carcinomas exhibit the “vascular pattern.”

### Portal Invasion by Tumors

The degree of portal invasion must be carefully assessed before surgery. Using MFI, it is possible to observe portal invasion in the early stages, as shown in Fig. 23.5 (see also Video 23.2). This image shows the leakage of portal vein blood in a pattern known as the “thread and streak sign,” in which small straight lines are seen in areas of portal invasion.

### Conclusion

Contrast-enhanced ultrasound (CEUS) is useful for navigation in surgery of the liver. In addition, liver metastases can be more accurately diagnosed before surgery. The clear depiction of such tumors including primary and metastatic tumors provides extremely valuable information before liver surgery. (As of 2013, in the United States, Sonazoid® is not approved by FDA).

## Intraoperative Ultrasound 3D Display Techniques and Cavity and FlyThru Methods

### Introduction

Various 3D display techniques have recently been introduced in the field of ultrasound diagnosis. Such 3D techniques, which provide images that depict structures more accurately

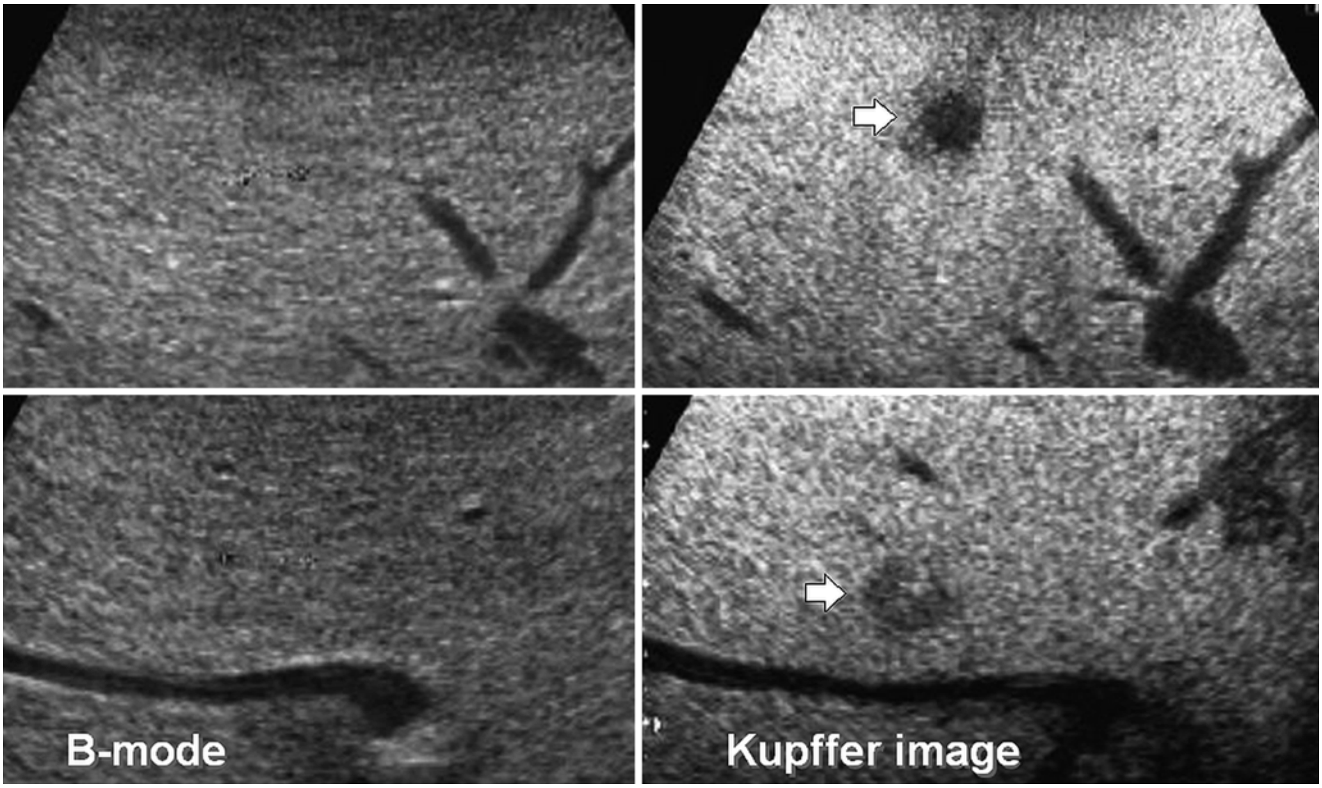


**Fig. 23.3** IOUS B-mode and Kupffer images showing liver metastases (*arrows*) from a pancreatic cancer. While these tumors are difficult to recognize by B-mode, these are readily detected by Kupffer images

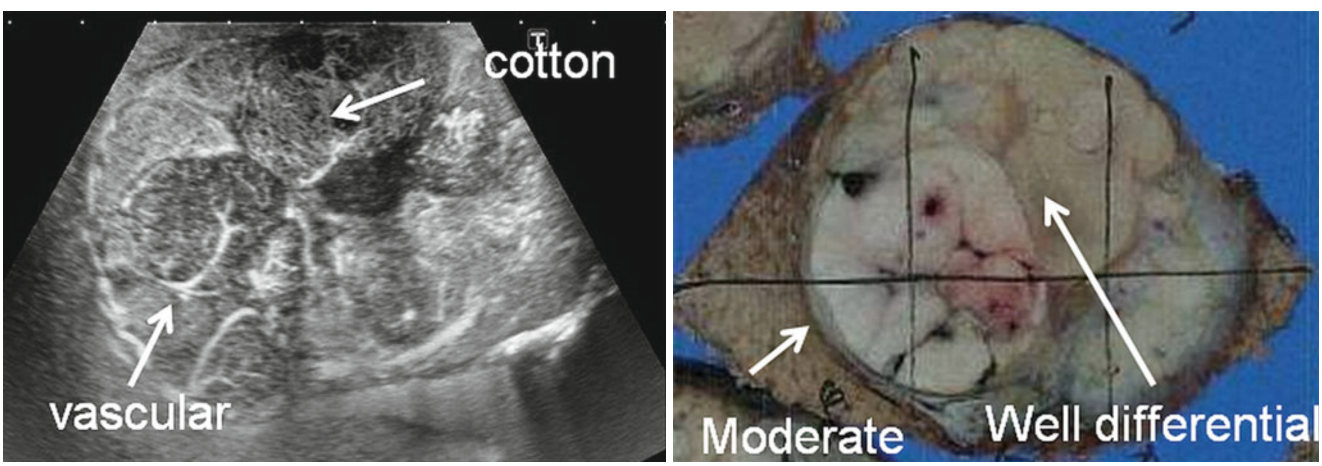


**Fig. 23.4** IOUS image of multinodular HCC (hepatoma) (*left*) and a section of corresponding area of a resected specimen (*right*). See also Video 23.1

than 2D images, have been clinically employed for the examination of the fetus, luminal structures in the abdomen, and the internal structure of the heart as well as for the evaluation of the cardiac valves and myocardium. In particular, recent advances in graphics workstations and computer graphics have led to the development of 3D display techniques for CT and MRI images, and 3D display is now employed proactively in clinical practice. Here, intraoperative ultrasound 3D display techniques and the cavity and FlyThru methods, which are based on virtual reality technology, are briefly discussed.

### How Are 3D Images Obtained?

Precisely determining the positions of the imaging planes is essential for accurately depicting 3D structures. Two techniques are available (Fig. 23.6): the matrix array (2D array)


**Fig. 23.5** IOUS image showing thread and streak sign in vascular MFI (micro-flow imaging). See also Video 23.2

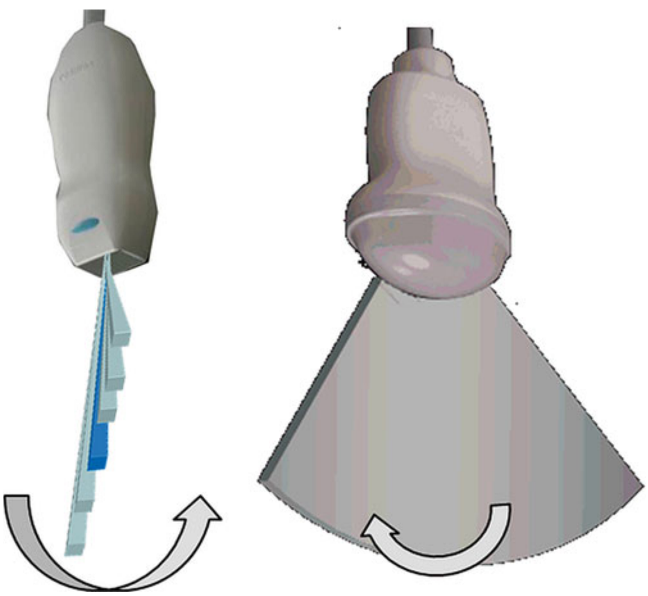

**Fig. 23.6** Acquisition method for 3D data. *Left*: 2D array method. *Right*: mechanical method

technique, which electronically aims the ultrasound beam in the desired direction, and the mechanical scanning technique, which swings the transducer elements of the 2D probe back and forth. The former technique requires advanced micromachining technology, complex electronic processing, and large-scale integrated circuits but controls beam acquisition electronically and provides a high degree of flexibility during scanning (Fig. 23.6, left). A major disadvantage of this technique is that the number of transducer elements and amount of circuitry required increases as the square of that for conventional systems, and systems employing this technique are therefore expensive. The latter technique can be implemented by combining existing technology and mechatronics, and the required circuitry can be incorporated by simply adding a mechanical control section to the standard 2D imaging circuits. This helps to control (save) the cost (Fig. 23.6, right). In both techniques, 3D information is obtained based on the ultrasound beams in the scanning field as shown in Fig. 23.6, and 3D images are reconstructed from this three-dimensionally extended fan-shaped ultrasound echo information.

## How Is 3D Information Displayed?

Details of the 3D information display (3D rendering) technique have been discussed elsewhere [1, 2], and therefore a brief summary of 3D rendering is provided here.

Multiplanar reconstruction (MPR) is the standard technique for displaying a 3D volume as slice images. In MPR, the three orthogonal planes in a 3D volume are displayed simultaneously as shown in Fig. 23.7 (see also Video 23.3). Normally, the plane of ultrasound scanning is defined as the A-plane; the scanning plane perpendicular to the A-plane is defined as the B-plane (i.e., the plane in which the transducer elements swing in the mechanical technique); and the plane perpendicular to both the A-plane and the B-plane is defined as the C-plane. Such images are intuitive and easy to interpret, but the simultaneously displayed area is limited, and it is therefore necessary to align the planes with the region of interest.

In the multiview method, many slice images at different slice positions in one of the MPR planes are displayed (Fig. 23.8) (see also Videos 23.4, 23.5, and 23.6). This is the basic 3D display method and is suitable for observing the 3D information in its entirety by selecting the desired display plane from among A, B, and C.

## What Is the Cavity Method?

In the cavity method, which is also referred to as the inversion method, the brightness of the image is inverted and the image is then displayed three-dimensionally so that areas of low brightness, such as the lumens of hollow structures, can be clearly visualized. This is useful for observing the overall luminal morphology and vascular structures (Fig. 23.9) (see also Video 23.7). When this method is employed for Kupffer imaging in contrast-enhanced ultrasound examinations, the positional relationships between a tumor and nearby vessels can be clearly observed in real time. This technique is expected to be useful for real-time navigation during surgical procedures.

## What Is the FlyThru Method?

The terms "fly-through" and "virtual endoscopy" have been used in 3D diagnostic imaging modalities such as CT and MRI. "Fly-through" refers to "flying through the human body," and virtual endoscopic 3D display in which the observer appears to be flying through luminal

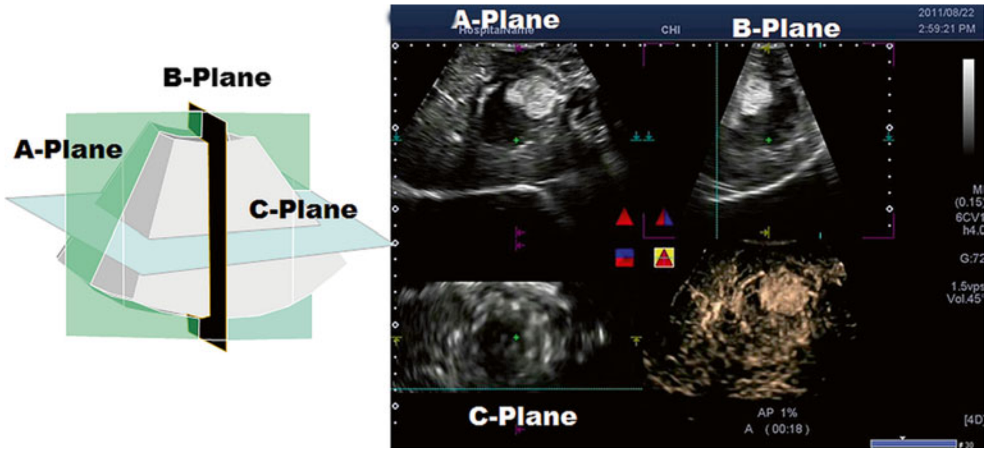


**Fig. 23.7** Three planes of 3D (*left*) and MPR (multi-planar reconstruction) display method in CEUS (*right*). See also Video 23.3

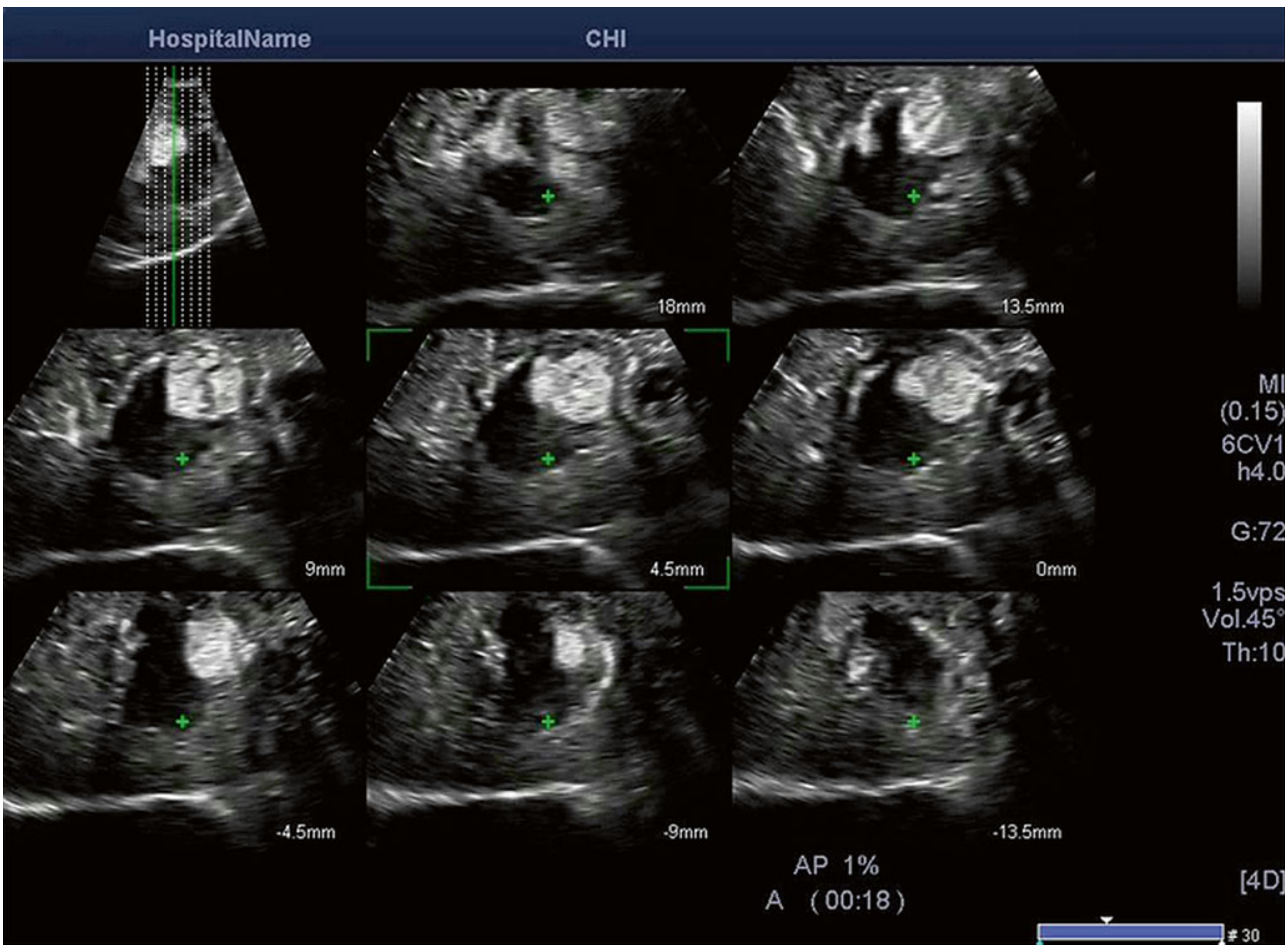


**Fig. 23.8** Multiview method (example of A-plane display): many slice images. See also Videos 23.4, 23.5, and 23.6 showing A-plane, B-plane, and C-plane

structures such as the trachea or blood vessels is known as FlyThru. This method makes it possible to observe the courses of luminal structures and blood vessels and also to detect the presence of plaque, protrusions (e.g., tumor invasion), or external compression from any desired viewpoint within the lumen. Examples of typical clinical applications are shown in Fig. 23.10 (see also Video 23.8 and 23.9).

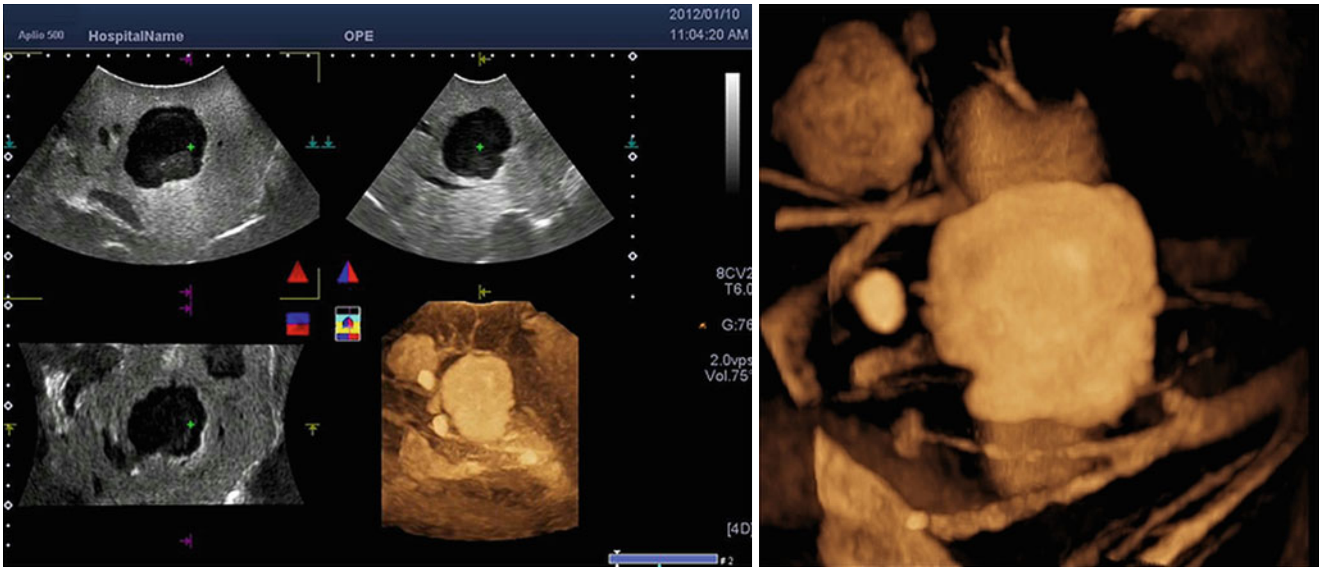


**Fig. 23.9** Cavity display in IOUS Kupffer imaging of metastases. See also Video 23.7. *Left*: multiview three planes and cavity display. *Right*: cavity display

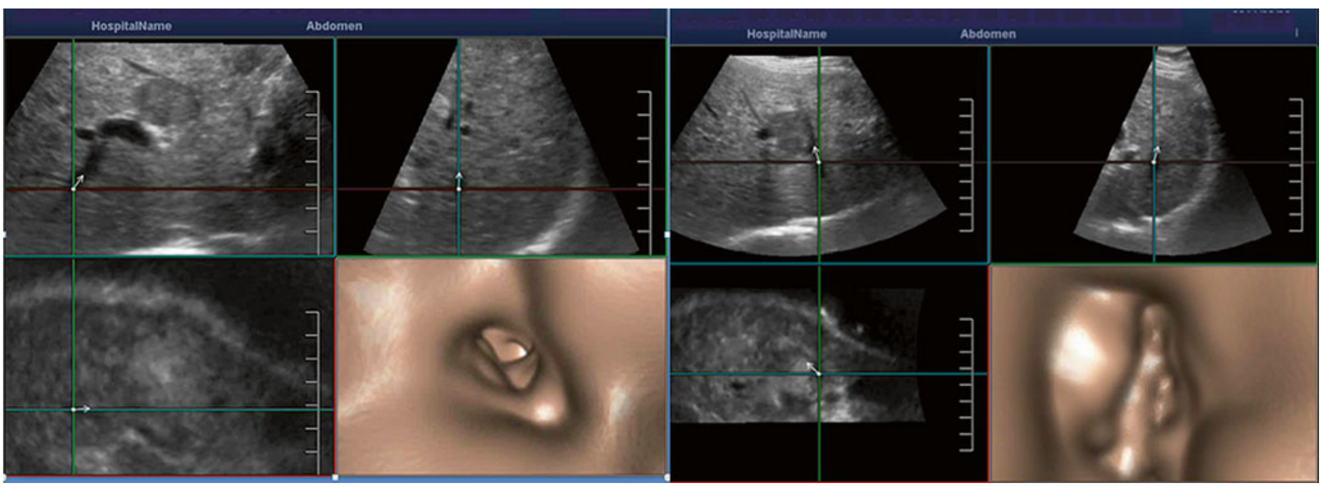


**Fig. 23.10** FlyThru display of HCC and portal and hepatic veins. See also Videos 23.8 and 23.9. *Left*: multiview three planes and FlyThru (right lower) of PV (portal vein). *Right*: multiview three planes and FlyThru (right lower) of HV (hepatic vein)

## Conclusion

The usefulness of 3D display in ultrasound has been discussed for many years. Cardiovascular examinations have led the way in the clinical application of 3D display, and the value of 3D display has been confirmed, particularly for the detailed evaluation of the cardiac valves. The value of 3D has also been confirmed in its application to obstetric examinations. Recently, with the development of 2D array technology, new 3D display techniques with improved real-time performance characteristics are being explored.

## Fusion Technique for Combining Ultrasound with CT and MR

### Introduction

The fusion technique allows the volume-to-volume fusion of images acquired by two different modalities. Real-time ultrasound images can be viewed in the same cross-sectional planes as in previously acquired CT or MR volume data. This makes it possible to observe structures from the same locations and to navigate in the region of interest. The fusion

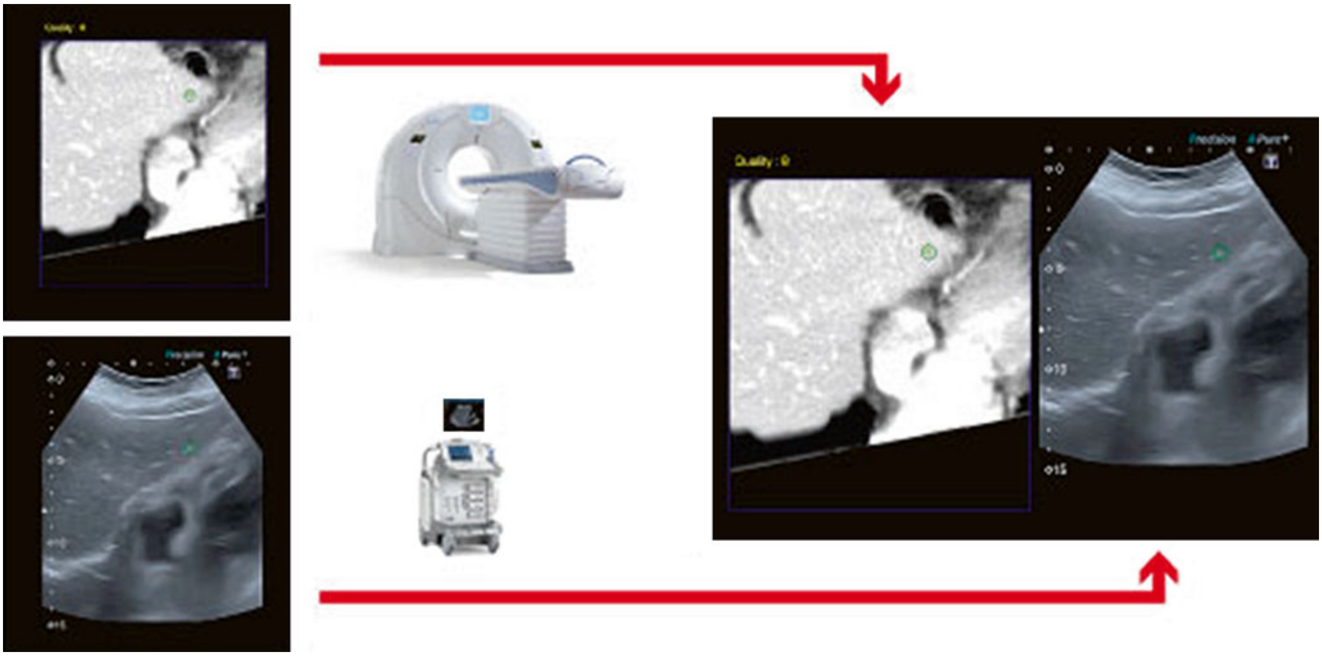

**Fig. 23.11** Fusion technology. The fusion technique displays both a CT image and an ultrasound image simultaneously

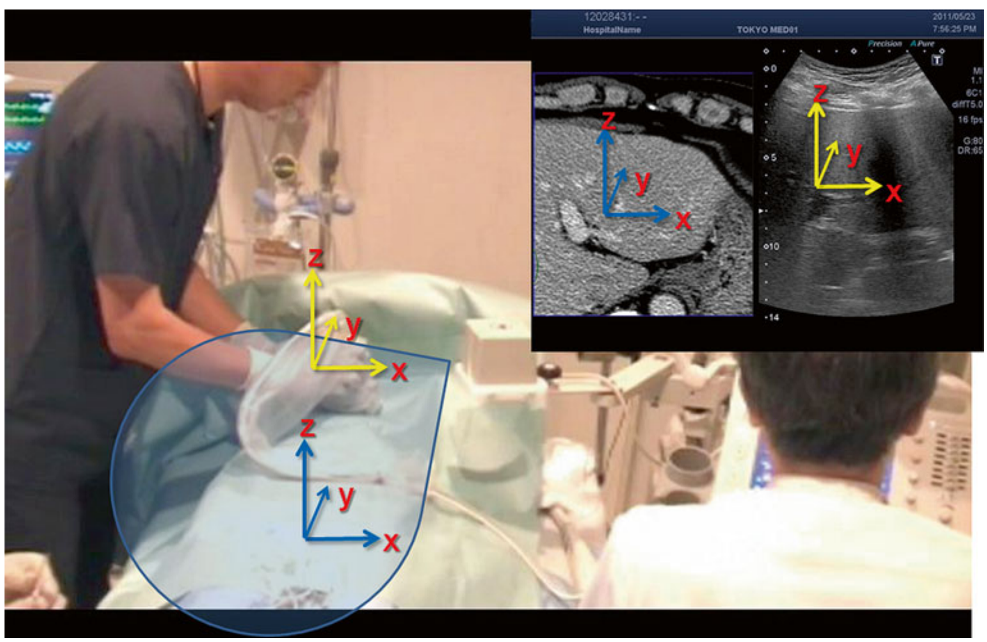


**Fig. 23.12** Setting up the directions in both images (axes lock)

technique reads 3D DICOM datasets from all major imaging modalities and displays the corresponding images in real time next to the live ultrasound display, as shown in Fig. 23.11. To permit comprehensive pre- and post-intervention evaluation, Smart Fusion is available in all ultrasound imaging modes, including color Doppler and contrast-enhanced ultrasound.

### Easy Setup

Image alignment is required in order to synchronize the ultrasound images and CT/MR volumes. Figure 23.12 shows how the image directions are set using an ultrasound probe. A position sensor attached to the ultrasound probe receives position information from a magnetic field generator. After

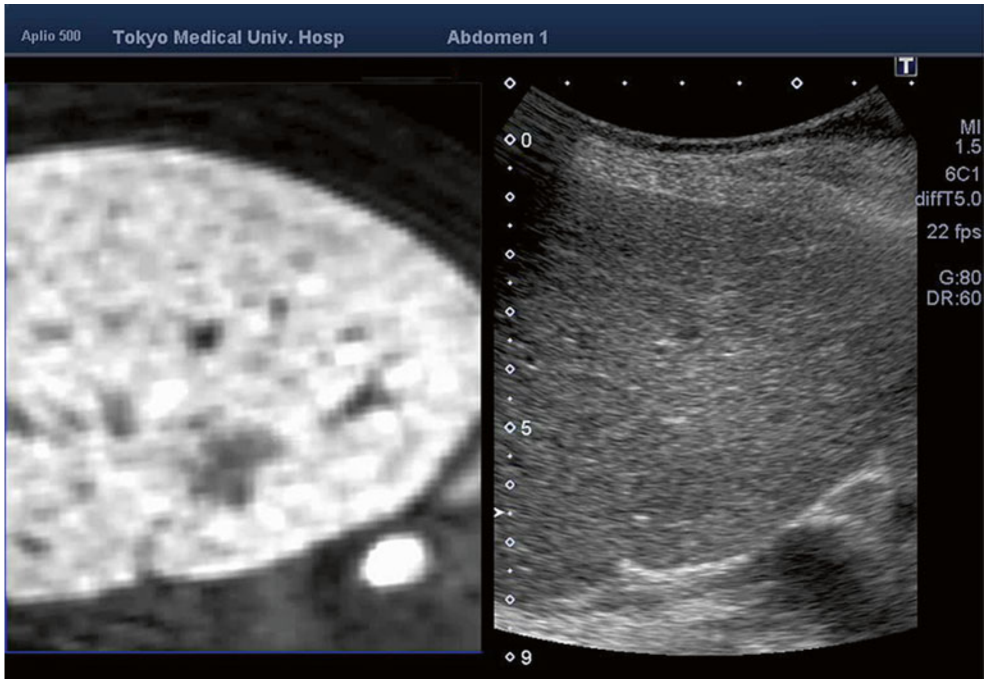


**Fig. 23.13** Smart fusion. EOB MRI (*left*) vs. B-mode US (*right*)

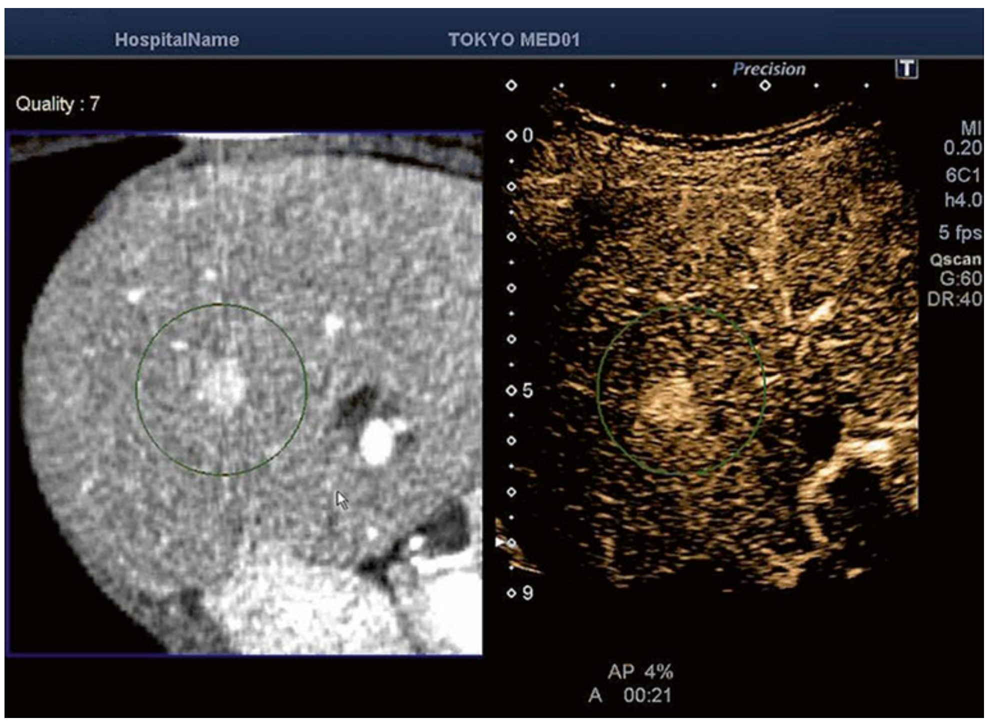


**Fig. 23.14** Fusion. CTA vs. CEUS (Sonazoid®). See also Video 23.10. CTA (*left*) and CEUS (*right*) showing enhancement of a tumor (*circle area*) by CEUS

setup, the ultrasound image and the CT or MR image are precisely synchronized, and after synchronization, the positions of the images are adjusted automatically.

### Diagnostic Applications

Ultrasound is useful for characterizing focal lesions, but it suffers from a number of limitations such as artifacts, acoustic shadowing, and attenuation. CT and MRI are the standard modalities for evaluating patients in clinical practice, particularly in the preoperative settings. Ultrasound has the advantages of lower cost and no radiation exposure, but the disadvantage of operator dependency. The fusion technique can be used to observe multiple lesions within a solid organ. Figure 23.13 shows an example of synchronization. Contrast-enhanced MR imaging with EOB (Gd-EOB-DTPA) clearly shows the location of the tumor, but on the other hand, the tumor is difficult to observe in the ultrasound image. This technique is helpful for the localization in addition to the diagnosis and characterization of tumors. Figure 23.14 (see also Video 23.10) shows an example of

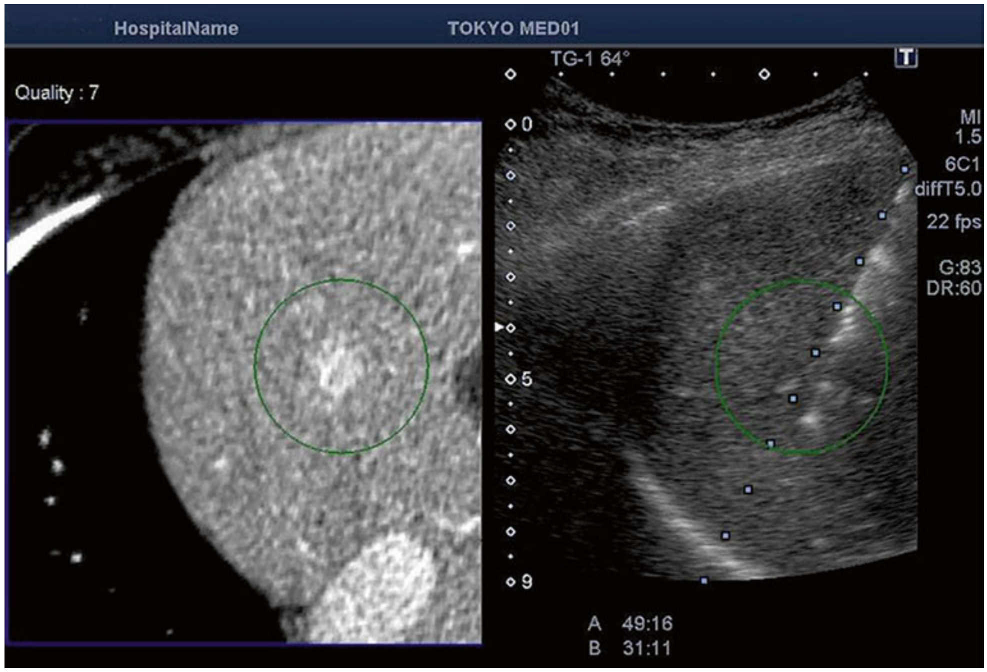


**Fig. 23.15** Fusion. CTA vs. RFA (RITATM) puncture. See also Video 23.11. CTA (*left*) and CEUS (*right*). CTA shows an enhanced (hyperdense) tumor (*circle*), while CEUS shows a puncture of an RFA needle into a hypoechoic tumor (*circle*)

synchronization between CTA and CEUS in the arterial phase. This is useful for estimating the margins of the area to be ablated.

### Interventional Applications

The fusion technique is useful in interventional applications because it reduces procedure times and provides a more accurate treatment. From a technical point of view, the fusion technique allows different access points and orientations to be used, which is not possible with CT or MR. Figure 23.15 (see also Video 23.11) shows real-time puncture of an RFA (radiofrequency ablation) needle using the fusion technique.

### Conclusion

Matching the transducer position with previously acquired 3D datasets is a simple and quick two-step process. By moving the transducer over the region of interest, it is possible to browse through the region in both real-time ultrasound images and previously acquired volume data simultaneously. In addition, intelligent target and marker points can be set to facilitate navigation in the region of interest during surgical or interventional treatment.

## Elastic Imaging: Elastography

### Introduction

Physicians commonly employ palpation as an important diagnostic technique in the examination of various organs such as the breast, thyroid gland, liver, and digestive tract. When an organ is palpated, malignant tumors feel more rigid (firmer, harder) than benign lesions. This physical characteristic is related to their elastic properties. Important causes of an increase in tissue stiffness are tissue transformation, fibrosis, and steatosis. Ultrasound elastography is expected to be a useful adjunct technology for the detection of tumors, for the precise determination of the extent of cancer such as breast cancer, for the differential diagnosis and confirmation of benign and malignant lesions, and for guidance during biopsy procedures. More accurate targeting of biopsies helps to increase specificity. With regard to the prostate gland, this significantly reduces the number of biopsies required in an individual patient.

### Basic Theory of Ultrasound Elastography

There are two methods for measuring the stiffness of a tumor: the strain method and the shear wave method [3].

### Strain Method

There is a relationship between the amount of applied force and the degree of deformation. Two quantitative values are related to each other: pressure and strain. When force is applied to a tumor, it will deform. The relative amount of tissue distortion is called strain. The strain rate is defined as shown in Fig. 23.16.

Figure 23.16 shows the relative stiffness of the hard and soft components at the same pressure. Compression (stress) is manually applied to the tissues, and the values with and without compression are compared. In real-time ultrasound elastography, mild pressure is applied. The lesion is positioned at the center of the region of interest (ROI), and the transducer is pressed and released 3–5 times using mild pressure. It is important to ensure that pressure is applied vertically and that the target is centered and does not shift out of the scan plane.

A strain (elasticity) image is obtained by comparing the tissue data acquired in a selected ROI with and without compression. The degree of tissue distortion (strain) is measured by real-time imaging and displayed as a color-coded image. Figure 23.17 shows a typical screen display in strain elastography.

### Shear Wave Method

Shear wave elastography is another method for obtaining elasticity images. It is based on the combination of the radiation force induced in the tissues by the ultrasound beam and a fast imaging sequence that displays the propagation of the resulting shear waves in real time.

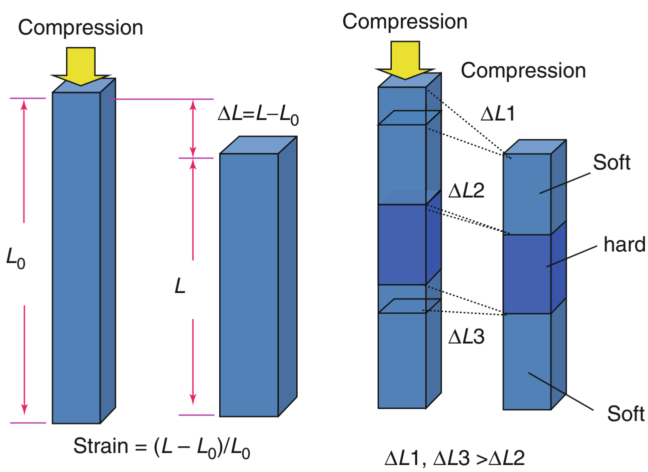


**Fig. 23.16** Relationship between compression value and strain

This radiation force or "push pulse" consists of focused beams of acoustic energy (ultrasound) and is generated by the probe, unlike the manual compression technique. The shear waves, or transverse waves, move in a perpendicular manner (i.e., motion is perpendicular to the direction of wave propagation). Figure 23.18 shows the relationship between the push pulse and the shear waves.

### Clinical Applications

Elastography is used to evaluate the malignancy of tumors [4–6]. There are two methods for evaluating tumors. The first method is to determine the strain ratio between the tumor and tissues around the tumor, and the other method is to categorize the strain pattern of the tumor as an elasticity score (Tsukuba score).

Figure 23.19 shows a residual fibroadenoma of the breast examined using compressed strain imaging. It shows a typical benign appearance.

In shear wave elastography, the distribution of shear wave velocities can be observed in real time. The average velocity in the ROI can also be calculated.

Figure 23.20 shows an image of a hepatocellular carcinoma (HCC) obtained by intraoperative ultrasound (IOUS). It shows a typical color pattern and Young's modulus in the small ROI based on $E = 3\sigma Vs^2$.

The color scale indicates the value of Young's modulus (kPa). Red corresponds to hard tissues and blue corresponds to soft tissues, which is the opposite of the color scale in strain elastography.

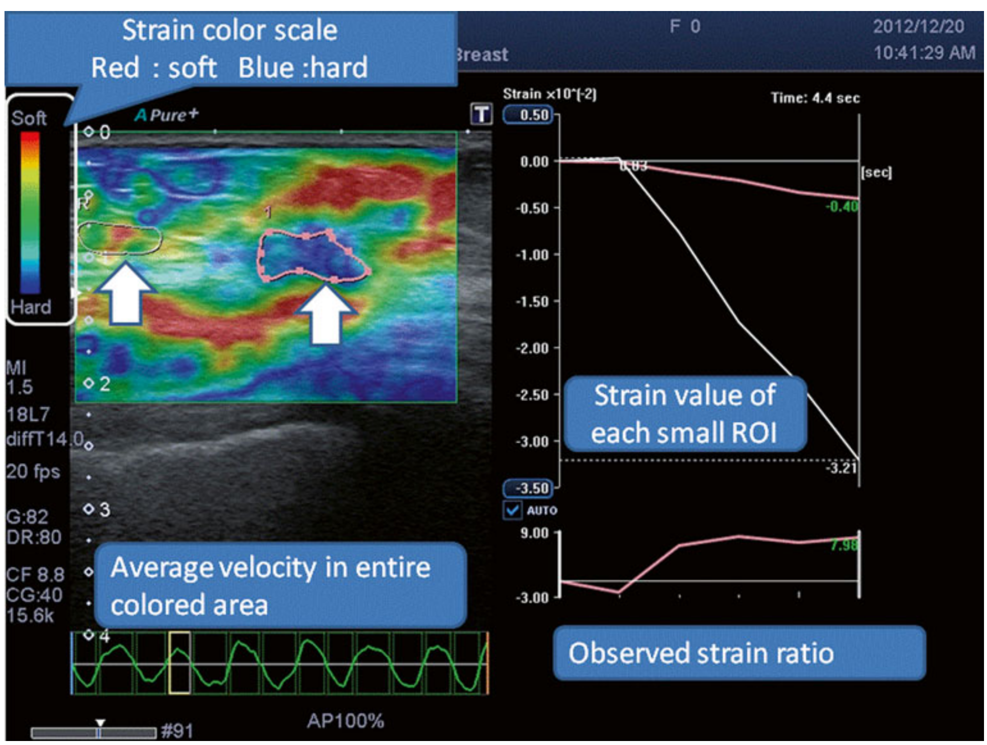


**Fig. 23.17** Typical screen display in strain elastography. Strain ratio of two ROIs (tumor and fat area) shows the location of malignant tumor. *Red* shows a soft area (fat), while *blue* shows a hard area (tumor)

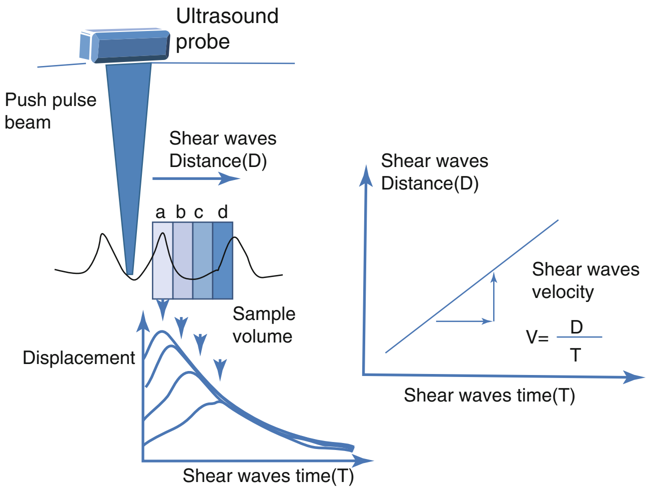


**Fig. 23.18** Push pulse and shear wave velocity of shear wave elastography

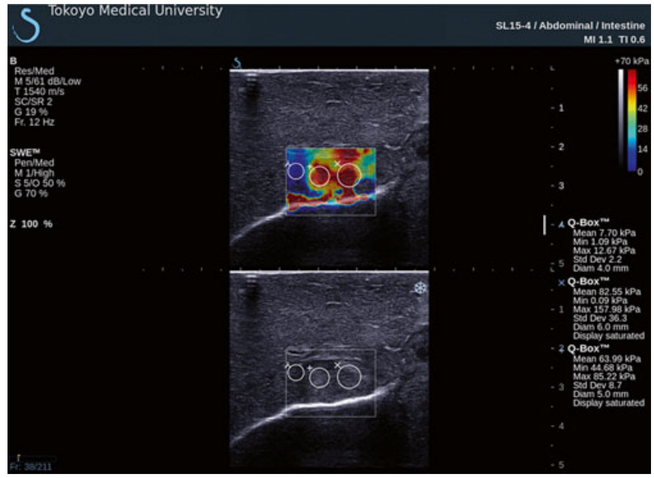


**Fig. 23.20** Clinical example of shear wave elastography (IOUS of HCC). *Red* shows large value of Young's modulus (hard) and *blue* shows small value. The center of tumor is observed as hard areas

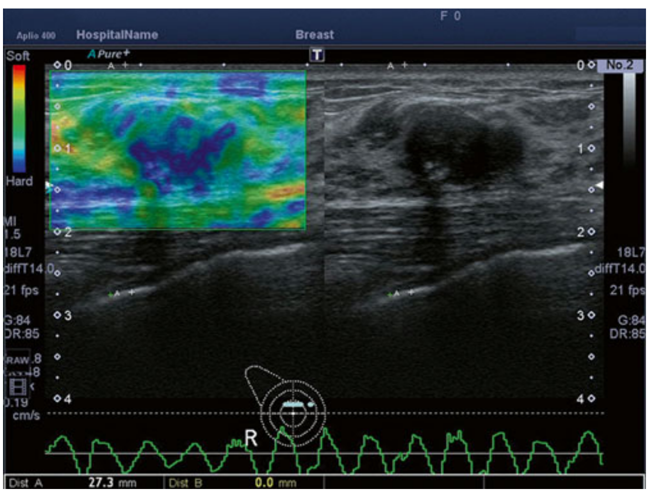


**Fig. 23.19** Clinical example of strain elastography (breast). Areas inside the tumor are seen to be hard (seen in *blue color*), which is the typical pattern for a benign breast tumor, fibroadenoma. Courtesy of Dr. Tokiko Endo (Nagoya Medical Center)

## Quantitative Ultrasound

### Introduction

Quantitative ultrasound (QUS) has been investigated for a long time, but its clinical use is very limited. Making tissue diagnosis by ultrasound, the so-called ultrasonic tissue characterization, cannot be achieved by B-mode imaging ultrasound alone. New ultrasound technology is required; in this chapter, potential QUS is briefly described based on our recent clinical investigation on the diagnosis of cancer in the lymph nodes.

### QUS for Lymph Node Metastases: Investigational Study

Detection of metastases in the lymph nodes (LN) is critical for cancer management. Conventional histopathological methods may overlook small metastatic foci because typically only one histological section is evaluated per LN. There are no current, practical means to evaluate LNs in their entire volume. As a result, clinically significant metastases may be missed.

A prospective study, funded in part by the National Institutes of Health and conducted at the University of Hawaii and Kuakini Medical Center in Hawaii and Riverside Research in New York, aims to create an operator-independent, fast, reliable system to scan and evaluate LNs in their entire volume utilizing high-frequency (HF) quantitative ultrasound (QUS). Over the past three decades, clinical applications of QUS have been investigated [7]. Unlike B-mode ultrasound images used clinically, HF QUS methods provide a quantitative means of estimating microscopic-scale tissue properties and are operator independent. Studies have further shown that HF QUS can effectively distinguish between metastatic and benign LNs [8, 9].

In this blinded study, freshly excised LNs were scanned at 26 MHz and echo-signal data were digitally acquired over the entire three-dimensional (3D) volume using a custom scanning system. LNs were step-sectioned at 50-μm intervals and stained with H&E and then later compared to 13 QUS parameters associated with tissue microstructures.

QUS parameters based on spectrum analysis and envelope statistics were estimated from the acquired RF echo-signal data [8, 9]. Linear-discriminant analysis classified LNs as metastatic or non-metastatic, and areas under receiver-operator characteristic curves (Az) were computed to assess classification performance. QUS-estimates and cancer-probability values derived from discriminant analysis were depicted in 3D images for comparison with 3D histology [10].

An interactive graphical user interface (GUI) was developed to permit virtual 3D dissection and exploration of freshly dissected LNs; the GUI displays linked, orthogonal, cross-sectional views of the node with a histology plane that matches the XY ultrasound plane. The interactive display consisted of a gray-scale B-mode plane of the 3D volume with overlaid color-encoded QUS-estimate or cancer-probability values. Cancer probabilities were estimated and color-coded for display using a Bayesian approach based on the discriminant score [10].

## Clinical Examples of QUS to Detect Lymph Node Metastases

Typical examples of clinical cases demonstrating the value of QUS in detecting macro- and micrometastases in lymph nodes are shown in Figs. 23.21 and 23.22 [10]: see legends of figures in details.

## Future Potential of QUS

Future in situ applications of these QUS methods will enable surgeons to identify suspicious axillary sentinel LNs of breast cancer patients in the operating room, in addition to non-sentinel axillary LNs. Additionally, intraoperative identification of suspicious LNs in situ by surgeons during colorectal and gastric cancer surgery may be possible. These QUS applications may contribute to more accurate staging, improving surgical treatment and management of breast, colorectal, and gastric cancer patients.

Future ex vivo applications will enable pathologists to identify suspicious LNs of breast, colorectal, and gastric cancer patients in the pathology lab. The number of regional LN metastases changes the node status of the tumor-node-metastases staging and therefore affects the cancer staging and prognosis in all three cancer types. This may contribute to more-sensitive detection of metastases and therefore more-accurate tumor-node-metastases staging by targeting the permanent histology section to the suspicious region.

These techniques and promising future devices may enable detection of the clinically relevant fraction of micrometastases that are missed by conventional single-section histology. The high probability of missed clinically significant metastases is of great concern because detection of all micrometastases is essential for accurate staging and effective treatment.

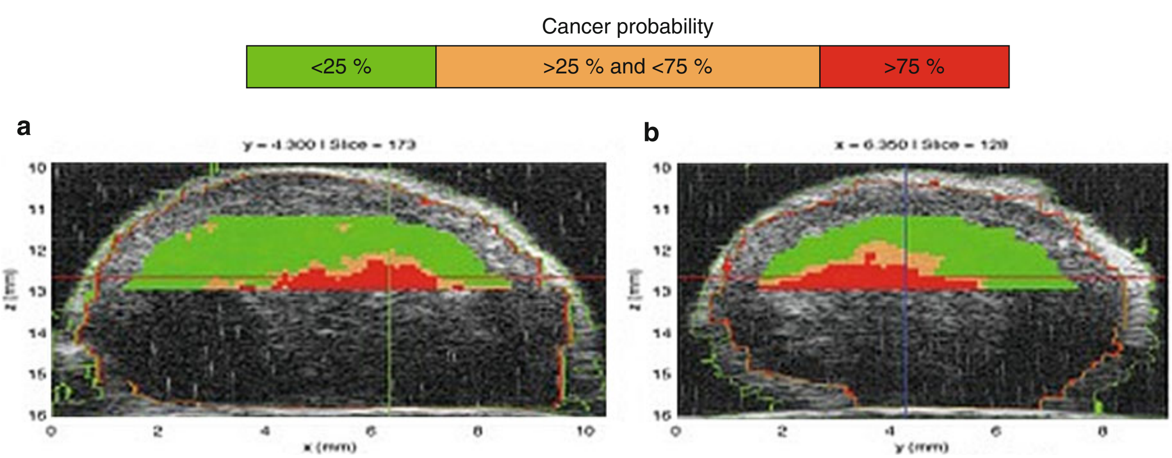


**Fig. 23.21** *Top* (**a**–**d**): 3D interactive GUI with cancer-probability images of a locoregional lymph node (LN) with partially metastatic adenocarcinoma from a patient with colorectal cancer. The LN is 9.54 mm in its largest dimension, and the metastasis is 5.09 mm in its largest dimension. The graphical user interface (GUI) displays three orthogonal gray-scale B-mode cross sections from a three-dimensional (3D) rendering in (**a**–**c**). The cross sections depict color-encoded cancer-probability values using *red* to indicate a probability greater than 75 %, *orange* to indicate a probability between 25 and 75 %, and *green* to indicate a probability less than 25 %. Figure (**d**) shows a co-registered hematoxylin and eosin (H&E)-stained histology photomicrograph that corresponds to the same section as in (**c**). These images show that excellent concurrence is achieved between the *red* cancer-probability region and the definitive histology result shown in (**d**) showing the demarcated metastatic tumor. *Bottom* (**e**–**h**): 3D interactive GUI with cancer-probability images of a benign locoregional lymph node (LN) from a patient with colorectal cancer. The LN is 4.41 mm in its largest dimension. The graphical user interface (GUI) displays three orthogonal gray-scale B-mode cross sections from a three-dimensional (3D) rendering in (**e**–**g**). (**h**) shows a co-registered hematoxylin and eosin (H&E)-stained histology photomicrograph that corresponds to the same section shown in (**g**). The cross sections depict color-encoded cancer-probability values using *red* to indicate a probability greater than 75 %, *orange* to indicate a probability between 25 and 75 %, and *green* to indicate a probability less than 25 %. These images show that excellent concurrence is achieved between the *green* (probably cancer-free) cancer-probability region and the definitive histology result of the benign LN shown in (**h**)

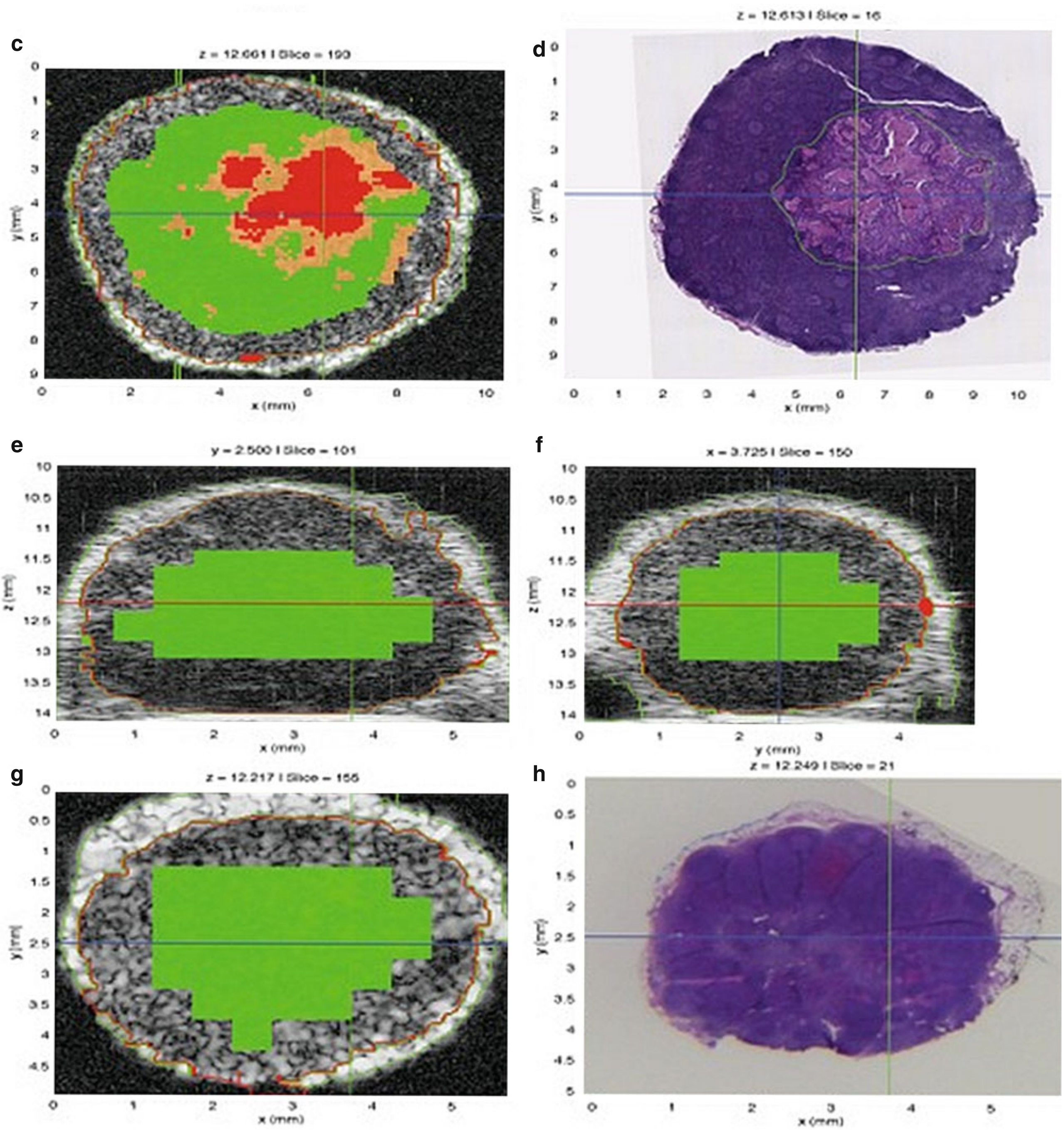


**Fig. 23.21** (continued)

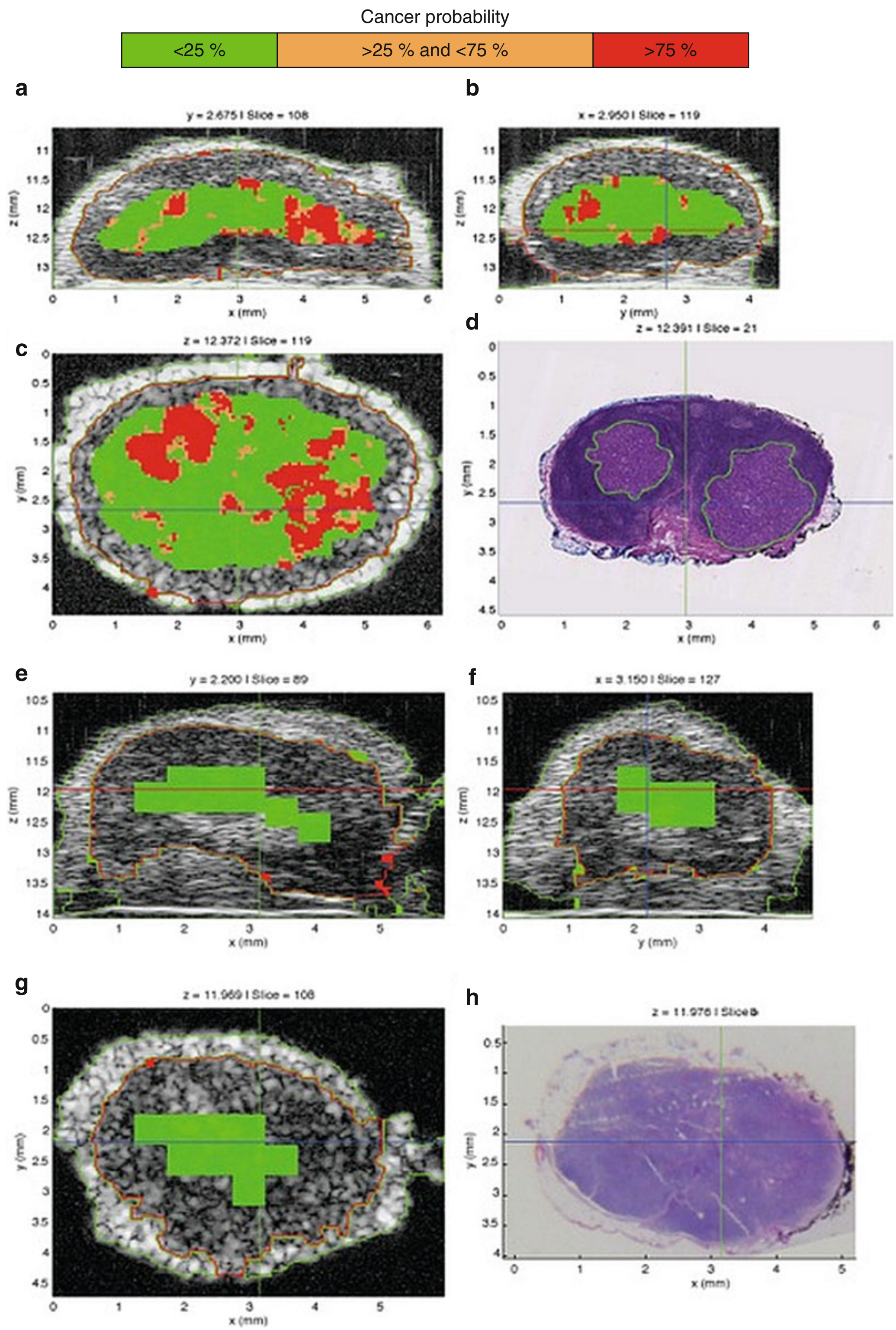


**Fig. 23.22** *Top* (**a**–**d**): Cancer-probability images of an axillary sentinel lymph node (LN) of an invasive ductal breast cancer patient. The LN is 5.86 mm in its largest dimension, and it contains two micrometastatic foci. The bigger focus is 1.82 mm in its largest dimension. The graphical user interface (GUI) displays three orthogonal gray-scale B-mode cross sections from a three-dimensional (3D) rendering in (**a**–**c**). The cross sections depict color-encoded cancer-probability values using *red* to indicate a probability greater than 75 %, *orange* to indicate a probability between 25 and 75 %, and *green* to indicate a probability less than 25 %. (**d**) shows a co-registered hematoxylin and eosin (H&E)-stained histology photomicrograph that corresponds to the same section shown in (**c**). Like Fig. 23.21, this figure shows excellent concurrence between the *red* high-probability region and the corresponding metastatic region in the histology result. *Bottom* (**e**–**h**): Cancer-probability images of a benign axillary sentinel lymph node (LN) of an invasive ductal breast cancer patient. The LN is 5.51 mm in its largest dimension. The cross sections depict color-encoded cancer-probability values using *red* to indicate a probability greater than 75 %, *orange* to indicate a probability between 25 and 75 %, and *green* to indicate a probability less than 25 %. Like Fig. 23.21, this figure (**e**–**g**) shows that excellent concurrence is achieved between the *green* cancer-probability region and the definitive histology result of the benign (cancer-free) LN shown in (**h**)

**Conclusions**

Abdominal ultrasound including TAUS, IOUS, LUS, and EUS can provide various types of diagnostic information which are otherwise not easily or practically available. In addition, ultrasound can guide or assist various surgical procedures in real time much easier than other imaging methods. Advantages of TAUS/IOUS/LUS, including high accuracy, safety, and speed, with comprehensive anatomical information, dynamic blood flow information, and real-time guidance capability, outweigh its disadvantages such as specific instrumentation requirement and slow learning curve. The use of abdominal ultrasound by surgeons is expected to increase along with more formal training in ultrasound for surgeons. New ultrasound technologies such as ultrasound contrast enhancement, 3/4-dimensional ultrasound, and others which are described in this chapter will be employed more during future abdominal ultrasound and will facilitate interventional procedures. Being like the surgeon's stethoscope and versatile transabdominally and intraoperatively, ultrasound is a valuable technique which is recommended to master for surgeons in various fields to improve surgical decision-making and surgical outcomes.

## References

1. Mitsunori Y, Tanaka S, Nakamura N, Ban D, et al. Contrast-enhanced intraoperative ultrasound for hepatocellular carcinoma: high sensitivity of diagnosis and therapeutic impact. J Hepatobiliary Pancreat Sci. 2013;20:234–42. Published online: 08 March 2012.
2. Arita J, Takahashi M, Hata S, Shindoh J, Beck Y, Sugawara Y, et al. Usefulness of contrast-enhanced intraoperative ultrasound using Sonazoid in patients with hepatocellular carcinoma. Ann Surg. 2011;254:992–9.
3. Ophir J, Céspedes I, Ponnekanti H, et al. Elastography: a quantitative method for imaging the elasticity of biological tissues. Ultrason Imaging. 1991;13:111–34.
4. Itoh A, Ueno E, Tohno E, et al. Breast disease: clinical application of US elastography for diagnosis. Radiology. 2006;239(2):341–50.
5. Fischer T, Peisker U, Fiedor S, et al. Significant differentiation of focal breast lesions: raw data-based calculation of strain ratio. Ultraschall in der Medizin. 2012;33(4):372–9.
6. Tanter M, Bercoff J, Athanasiou A, et al. Quantitative assessment of breast lesion viscoelasticity: initial clinical results using supersonic shear wave imaging. Ultrasound Med Biol. 2008;34:1373–86.
7. Lizzi FL, Greenebaum M, Feleppa EJ, Elbaum M, Coleman DJ. Theoretical framework for spectrum analysis in ultrasonic tissue characterization. J Acoust Soc Am. 1983;73:1366–73.
8. Mamou J, Coron A, Hata M, Machi J, Yanagihara E, Laugier P, Feleppa EJ. Three-dimensional high-frequency characterization of cancerous lymph nodes. Ultrasound Med Biol. 2010;36:361–75.
9. Mamou J, Coron A, Oelze M, Saegusa-Beecroft E, Hata M, Lee P, Machi J, Yanagihara E, Laugier P, Feleppa EJ. Three-dimensional high-frequency backscatter and envelope quantification of cancerous human lymph nodes. Ultrasound Med Biol. 2011;37:345–57.
10. Saegusa-Beecroft E, Machi J, Mamou J, Hata M, Coron A, Yanagihara E, Yamaguchi T, Oelze M, Laugier P, Feleppa E. 3D quantitative ultrasound for detecting lymph-node metastases. J Surg Res. 2013;183:258–69.